SOILS AND FOUNDATIONS Vol. 38, No. 2, 179–190, June 1998
Japanese Geotechnical Society

THE PULL-OUT RESISTANCE OF MODEL SOIL NAILS

G. W. E. MILLIGAN[i] and KOUJI TEI[ii]

ABSTRACT

As an adjunct to a series of centrifuge model tests on nailed soil slopes, a comprehensive series of pull-out tests have been conducted on model nails. The objectives of the tests were to investigate the fundamental interaction mechanisms between nail and soil during pull-out, and to obtain basic data needed for the analysis of the centrifuge tests. Three different soil types were used, all dry sands, and the parameters varied in the tests were the nail length and diameter, nail stiffness, and surface roughness of the nail.

Results of the tests are presented and considered in the context of a simplified theoretical model. The apparent coefficient of friction (bond) between stiff rough nails and soil is shown to be dependent on the friction angle of the soil, the rate of soil dilation during shear, the stiffness of the soil and the diameter of the nail in relation to the mean particle size of the soil. For smooth nails the bond resistance is much smaller, and such nails should not be used in practice. For relatively extensible nails the interaction mechanisms are complicated by the occurrence of progressive failure along the nail.

Key words: bond resistance, model tests, pull-out tests, soil nailing, soil reinforcement (**IGC**: E12)

INTRODUCTION

An extensive series of centrifuge model tests on nailed soil slopes has been conducted, using the centrifuge test facilities at City University. Because the nails were relatively short and strong, slope failures occurred as a result of pull-out of the nails rather than by their failure in tension or bending. To allow proper understanding and analysis of the tests, the pull-out resistance of the nails was studied in a subsidiary series of laboratory tests, the results of which are presented in this paper. Results of the centrifuge model tests are presented by Tei (1993).

Proper design of soil nailing requires an understanding of the interaction mechanism between the nails and the soil being reinforced. Bond resistance is developed by relative displacement of nail and soil, and may be investigated using pull-out tests. Soil-nail interaction is influenced by several factors, such as the properties of the soil, the roughness and stiffness of the nail and the boundary conditions of a test (Palmeira and Milligan (1989)). Furthermore, the change in stress on the nail due to dilatancy of the soil, when a nail is pulled out, makes the interaction mechanism very complicated and difficult to analyse (Schlosser and Guilloux, 1979). As pointed out by Dunham (1976) and Bolton (1990), pull-out tests of reinforcement tend to cause non-uniform strain and stress conditions both in the soil and the reinforcement, and hence require very careful interpretation.

Although the pull-out test has been one of the most convenient and popular means of obtaining the maximum pull-out resistance of a nail in both in-situ and model tests (Chang et al. (1977), Ingold and Templeman (1979), Murray et al. (1979)) no standard methods and configurations have been established. As the pull-out test is very sensitive to the test procedure and boundary conditions, care should be taken when comparing data obtained in different tests. However, when pull-out tests are carried out under well-controlled conditions, the results may provide fundamental and useful information regarding interaction mechanisms.

In this research programme a number of pull-out tests, direct shear tests of sand, and interface tests between sand and reinforcement were performed in order to:

(1) investigate the interaction mechanism between a nail and soil,
(2) quantify the influence of various parameters on the apparent friction coefficient (bond) between nail and soil, and
(3) obtain basic data for analyzing the results of centrifuge model tests of nailed slopes.

[i] Associate, Geotechnical Consulting Group, 1[A] Queensberry place, London SW7 2DL, UK. (Formerly University Lecturer, Department of Engineering Science, University of Oxford, UK)
[ii] Senior Geotechnical Engineer, Civil Works Technology Department, Tokyu Construction Co., Ltd., 1-15-21 Shibuya, Shibuya-ku Tokyo 150-0002, (Formerly Research Student, Department of Engineering Science, University of Oxford, UK)
Manuscript was received for review on October 25, 1996.
Written discussions on this paper should be submitted before January 1, 1999 to the Japanese Geotechnical Society, Sugayama Bldg. 4F, Kanda Awaji-cho 2-23, Chiyoda-ku, Tokyo 101-0063, Japan. Upon request the closing date may be extended one month.

DIRECT SHEAR TESTS AND INTERFACE TESTS

Apparatus

A medium size direct shear test apparatus originally made by Jewell (1980) was used to carry out the direct shear tests on the sand (Fig. 1). The box had a plan area of 254 mm × 153 mm and a sample depth of about 150 mm. The top platen of the shear box was fixed to the top half of the shear box; thus it had symmetrical upper and lower boundary conditions, which tends to eliminate the rotation of the box during shearing (Airey, 1987; Jewell, 1989).

The shear load S was applied by a ram driven at a constant speed of 0.08 mm/min by an electric motor. The ram pushed the bottom half of the shear box, which was free to run on bearings; the top half providing resistance to movement by reacting against a deflector bar. Measurements of the central deflection of the bar gave the shear load to an accuracy of about 1 N. Because of the relatively large plan area of the shear box and the use of a hanger system to apply the vertical load, the maximum vertical stress σ_v was limited to about 60 kPa. Generally, the sample was sheared to a displacement of 4 mm. The shear displacement X and the dilation Y were measured by means of dial gauges with a sensitivity of ±0.01 mm.

Sand

Two standard yellow Leighton Buzzard Sands, 14/25 and 50/100, were used. These are uniform quartz laboratory sands with sub-angular particles. The reference numbers refer to two old British Standard sieve sizes; the sand passes the first but is retained by the second. Details of the sands are given in Table 1. The sand was placed in the test box by pluviation from a hopper, the density being controlled by varying the deposition rate through different perforated plates. Fuller details of the test preparation method are given by Tei (1993).

Results of a series of direct shear tests at a vertical stress of 36 kPa are shown in Fig. 2. The results for 14/25 dense sand are in good agreement with those reported by Jewell and Wroth (1987) and Pedley (1991) using the same apparatus.

The measured peak shearing resistances are also presented in Table 1, where the angle of dilation ψ and the peak direct shear friction angle ϕ_{ds} of the soil are given by:

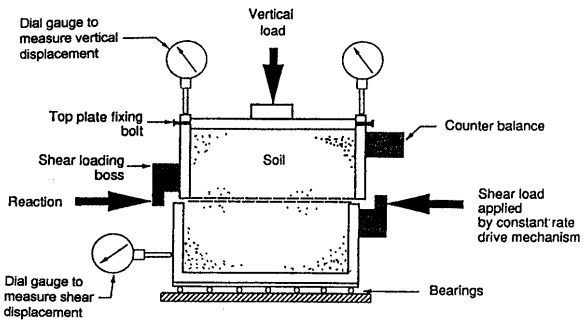

Fig. 1. General arrangement of medium-sized shear box

Table 1. Details of test sands

		50/100 yellow L.B. sand		14/25 yellow L.B. sand
G_s		2.65		2.65
e_{max}		0.89		0.79
e_{min}		0.57		0.49
$(\gamma_d)_{max}$	(kN/m^3)	16.65		17.50
Particle size	(mm)	0.15–0.20		0.6–1.18
D_{50}	(mm)	~0.18		~0.80
Density		Dense	Med. dense	Dense
Friction angle ϕ_{ds}	(Deg.)	39	36	48
Dilation angle ψ	(Deg.)	15	10	26
Interface friction δ	(Deg.)	30	26	32

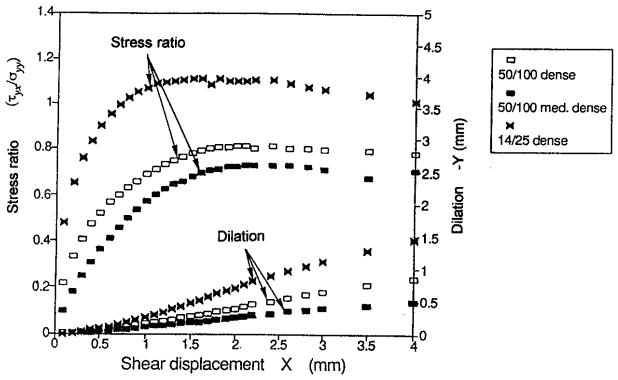

Fig. 2. Shear stress/displacement curves for shear box tests of Leighton Bizzard sands

$$\tan\psi = -\frac{\dot{\varepsilon}_{yy}}{\dot{\gamma}_{yx}} = \frac{dY}{dX} \tag{1}$$

$$\tan\phi_{ds} = \frac{\tau_{yx}}{\sigma_{yy}} \tag{2}$$

Interface Tests

The medium size box was also used to perform interface tests by installing the interface to be investigated at the level of the shear plane, in the lower half of the shear box, as shown in Fig. 3. An aluminium alloy plate, with sand glued to its upper surface to make it rough, was used for the interface material. Care was taken when placing the interface to ensure that no horizontal displacement of the interface occurred during the test. The upper half of the shear box was filled with the test sand and the interface test was carried out in a similar manner to a direct shear test. Peak interface friction angles are also given in Table 1. However it should be recognised that interface friction angles measured in a shear box may not

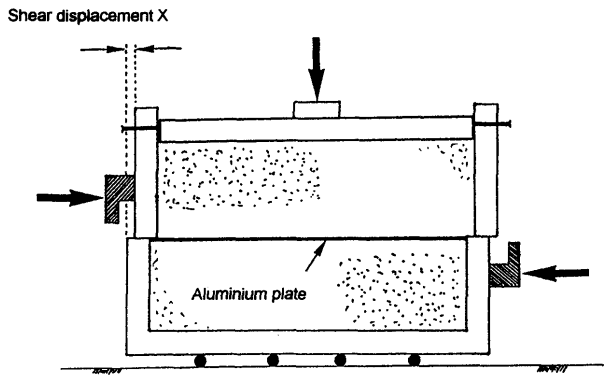

Fig. 3. General arrangement for interface tests

be applicable to the analysis of nail pull-out tests since the stress and strain regimes are very different. For full scale nails formed by grouting a borehole, the soil may be firmly bound to the grout at the interface so that any failure occurs within the soil, with the appropriate friction angle being the direct shear angle for the soil, ϕ_{ds}.

PULL-OUT TESTS-APPARATUS AND TEST PROCEDURE

The medium size direct shear box was modified to provide a displacement controlled pull-out test rig (Fig. 4). After a sufficient depth of sand had been deposited using a hopper, in the same way as in the direct shear tests, a nail was placed horizontally in the required position, 129 mm below the upper surface of the sand. The nail passed through a hole of 6 mm diameter in the front wall of the box and the head of the nail was firmly connected to a load cell, allowing measurement of the pull-out force. The rest of the sand was then rained in to the test box. The pull-out load was applied by a drive motor pulling the shear box on the roller bearings. This was opposite to the method of the conventional pull-out test in which the nail is pulled out while the test box remains stationary, but the relative displacement between soil and nail is the same in each system. Dial gauges measured the horizontal displacement of the box.

To minimize the adverse influence of the front wall (*see* Palmeira and Milligan, 1989), a small plastic tube, 70 mm long and 6 mm in diameter was firmly attached horizontally to the front wall of the box, to isolate the nail from the surrounding sand and ensure that there was no friction acting on that part of the length of the nail. Great care was taken not to bring the nail into contact with either the front wall or the small plastic tube during the sample preparation. Surcharge stresses of up to 55 kPa were applied to the top of the soil sample by weights on a hanger.

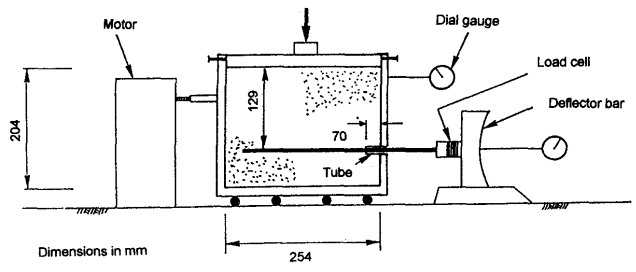

Fig. 4. General arrangement for pull-out tests

Two types of nail, stiff and extensible, with several different lengths, were prepared for the pull-out tests. Stiff nails were made of mild steel (elastic modulus $E_a=206\times10^6$ kPa) with circular cross section and diameters $D=1.0$, 1.4, 2.0, 2.6, 3.2, 4.0 and 5.2 mm. Extensible nails were made of a rubber tube with external diameter $D_e=3.0$ mm and internal diameter $D_i=2.0$ mm. The elastic modulus of the rubber tube was measured in uniaxial tension tests as $E_a=0.02$ kN/m^2.

Three main parameters for the nail were varied in the pull-out tests; roughness (smooth and rough), extensibility (stiff and extensible) and diameter D. A rough nail was made by gluing sand on the surface of the corresponding smooth nail, increasing the diameter by 0.7 mm for 50/100 sand and 2.0 mm for 14/25 sand.

RESULTS OF PULL-OUT TESTS

Pull-out Tests of Stiff Nails with a Rough Surface

Out of the total of 51 tests with uninstrumented nails, 38 pull-out tests were performed on stiff-rough nails. Specific details, together with some results of the tests, are given in Table 2. In the table, μ^* is the friction coefficient, defined by

$$\mu^*=\frac{f^*}{\tan\phi_{ds}} \tag{3}$$

where f^* is the apparent friction coefficient given by μ_{max}/σ_m, where τ_{max} and σ_m are the maximum shear stress and the initial mean normal stress on the nail respectively. The value of τ_{max} is given by

$$\tau_{max}=\frac{F_p}{\pi Dl} \tag{4}$$

where F_p is the peak pull-out force, D the diameter of the nail and l its embedded length. The mean stress is taken to be given by

$$\sigma_m=\frac{(1+K_0)}{2}\sigma_v \tag{5}$$

with $K_0=1-\sin\phi_{ps}$, K_0 being the coefficient of earth pressure at rest and ϕ_{ps} the plane strain angle of friction for the soil. The values of σ_v include the self weight of soil above the nail. In calculating the embedded nail length at any stage of the test, a correction was made to the measured displacement of the box for the elastic extension of the free length of the nail.

Typical load-pullout displacement results for stiff-rough nails are shown in Fig. 5, together with results of unreinforced direct shear tests for the corresponding sands with nearly the same relative densities. Important features of the results are:-

Table 2. Details of pull-out tests with stiff rough nails

Test	Nail length l (mm)	Diameter D (mm)	Surcharge σ_v (kPa)	Peak force F_p (N)	f^*	μ^*
Tests with dense 50/100 L.B. sand						
R1-1	200	1.7	22.7	44.9	2.81	3.47
R1-2	200	2.1	22.7	54.3	2.75	3.40
R1-3	200	2.7	22.7	63.8	2.51	3.10
R1-4	200	3.3	22.7	76.1	2.45	3.02
R1-5	200	3.9	22.7	86.2	2.35	2.90
R1-6	200	4.7	22.7	96.8	2.19	2.70
R1-7	200	5.9	22.7	111.6	2.01	2.48
R1-8	180	1.7	22.7	39.0	2.71	3.35
R1-9	150	1.7	22.7	33.2	2.77	3.42
R1-10	90	1.7	22.7	19.1	2.66	3.28
R1-11	200	1.7	5.6	11.9	3.00	3.70
R1-12	200	1.7	11.0	22.7	2.93	3.62
R1-13	200	1.7	16.2	32.5	2.85	3.52
Tests with medium dense 50/100 L.B. sand						
R2-1	200	1.7	22.0	32.4	2.03	2.80
R2-2	200	2.1	22.0	36.9	1.87	2.58
R2-3	200	2.7	22.0	26.2	1.82	2.50
R2-4	200	3.3	22.0	54.3	1.75	2.41
R2-5	200	3.9	22.0	61.2	1.67	2.30
R2-6	200	4.7	22.0	72.0	1.63	2.24
R2-7	200	5.9	22.0	85.9	1.55	2.14
R2-8	180	1.7	22.0	28.5	1.98	2.73
R2-9	150	1.7	22.0	24.9	2.08	2.86
R2-10	90	1.7	22.0	14.2	1.98	2.72
R2-11	200	1.7	6.7	9.8	2.01	2.76
R2-12	200	1.7	10.3	15.3	2.04	2.81
R2-13	200	1.7	15.5	22.7	2.02	2.78
Tests with dense 14/25 L.B. sand						
R3-1	200	3.0	23.2	107.5	4.10	3.69
R3-2	200	3.5	23.2	111.9	3.92	3.53
R3-3	200	3.9	23.2	131.6	3.86	3.48
R3-4	200	4.4	23.2	146.6	3.81	3.43
R3-5	200	5.0	23.2	160.4	3.67	3.30
R3-6	200	5.8	23.2	184.6	3.64	3.28
R3-7	180	3.0	23.2	96.8	4.10	3.69
R3-8	150	3.0	23.2	82.6	4.20	3.78
R3-9	90	3.0	23.2	47.9	4.06	3.66
R3-10	200	3.0	16.7	77.2	4.09	3.68
R3-11	200	3.0	11.5	54.3	4.18	3.76
R3-12	200	3.0	6.1	27.9	4.04	3.64

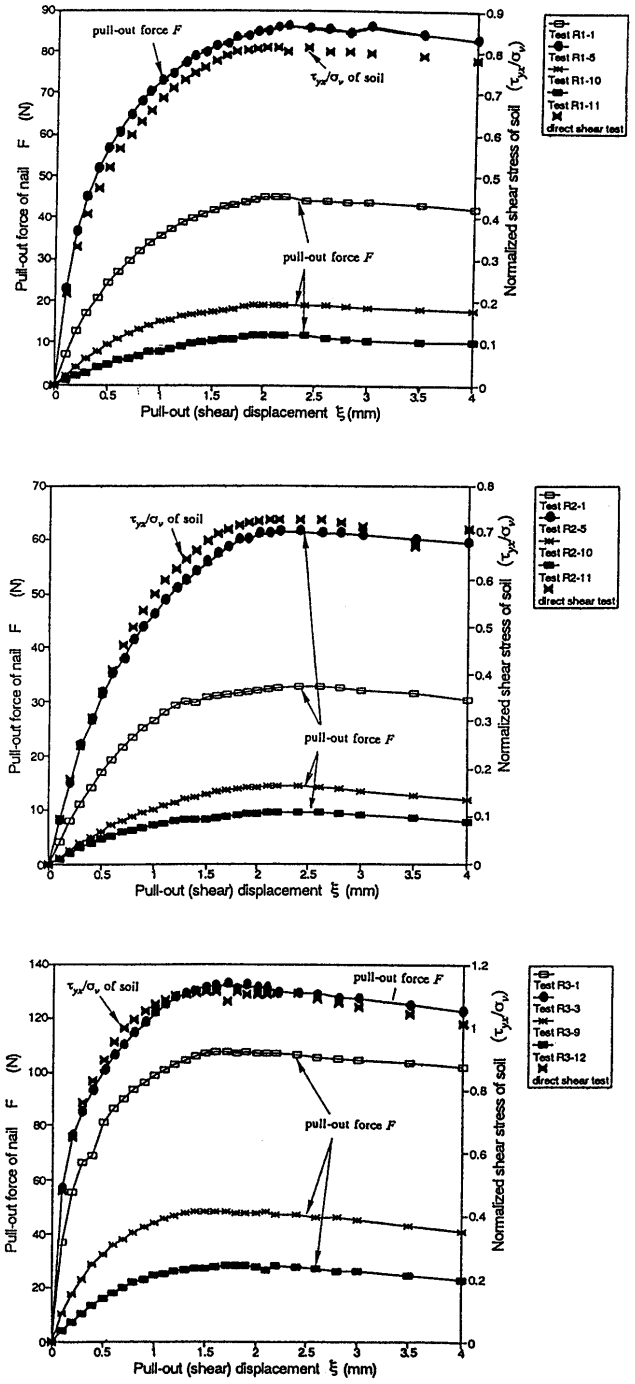

Fig. 5. Force/displacement curves for pull-out tests with stiff rough nails

(1) up to peak, the pull-out curves are approximated by hyperbolae and of similar form to the load-displacement curve for unreinforced direct shear tests of the sand;

(2) ξ_p, the pull-out displacements of a nail required to mobilize the peak pull-out force F_p, were almost the same irrespective of diameter D, initial length l_i and vertical stress σ_v. The displacements for each of the sands were:-

$\xi \approx 2.0$ mm for 50/100 dense sand, Fig. 5(a)

≈ 2.2 mm for 50/100 medium dense sand, Fig.

5(b)
≈1.5 mm for 14/25 dense sand, Fig. 5(c)
These are also very similar to the horizontal displacements at peak stress ratio in the direct shear tests of the three sands, as shown in Fig. 2 and also in Fig. 5. Schlosser (1990) and Bergado et al. (1992) have pointed out that, in general, displacements of 1 to 5 mm are required to mobilise the peak pull-out force F_p.

(3) after peak, the pull-out force was observed to decrease gradually, at least up to a displacement of 4.0 mm, the maximum value reached in these tests.

(4) peak pull-out force F_p increased as the shear strength of the soil increased, indicating that the friction angle of the sand plays an important role.

In addition to the above tests, three tests were carried out on nails instrumented to measure the axial stress distributions at the peak pull-out force F_p for 50/100 dense sand with surcharge stresses σ_v=5.6, 11.0 and 22.7 kPa. Ten strain gauges were used to instrument the nail in pairs at different positions along the length of the nail. The nail was made of stainless steel tube, of total length l=12.0 cm and external and internal diameters D_e=2.0 mm and D_i=1.9 mm, respectively. The results are shown in Fig. 6; fairly linear axial stress distributions $\sigma(x)/\sigma_0$ along the nail were observed in these tests, where σ_0 is the axial stress at the head of the nail (x=0) at the front wall.

Apparent friction coefficients from tests on nails of different lengths and with different vertical stresses in the sand are summarised in Fig. 7. It appears that neither nail length nor vertical stress has a significant influence on pull-out behaviour, at least within the range of values used in the tests.

Pull-out Tests of Stiff Nails with a Smooth Surface

Details of tests using stiff smooth nails are given in Table 3. The load-displacement results for stiff-smooth nails for 50/100 dense and 14/25 dense Leighton Buzzard Sand are shown in Fig. 8. For all tests with smooth nails, the initial length of the nail was 200 mm

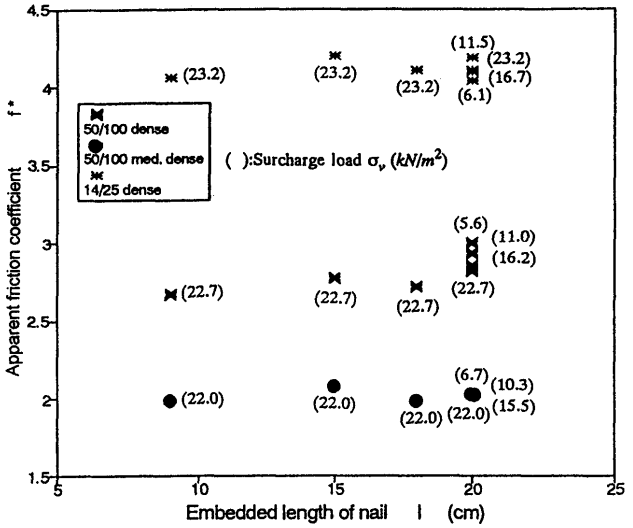

Fig. 7. **Pull-out tests of stiff rough nails: influence of length and stress level**

Table 3. Details of pull-out tests with stiff smooth nails

Test	Nail length l (mm)	Diameter D (mm)	Surcharge σ_v (kPa)	Peak force F_p (N)	f^*	μ^*
Tests with dense 50/100 L.B. sand						
S1-1	200	2.0	22.7	4.9	0.26	0.32
S1-2	200	2.6	22.7	6.6	0.27	0.33
S1-3	200	3.2	22.7	7.7	0.26	0.32
S1-4	200	4.0	22.7	9.9	0.26	0.32
S1-5	200	5.2	22.7	12.7	0.26	0.32
Tests with dense 14/25 L.B. sand						
S2-1	200	2.0	23.2	5.7	0.33	0.30
S2-2	200	2.6	23.2	7.0	0.31	0.28
S2-3	200	3.2	23.2	9.0	0.32	0.29
S2-4	200	4.0	23.2	11.1	0.32	0.29
S2-5	200	5.2	23.2	14.6	0.32	0.29

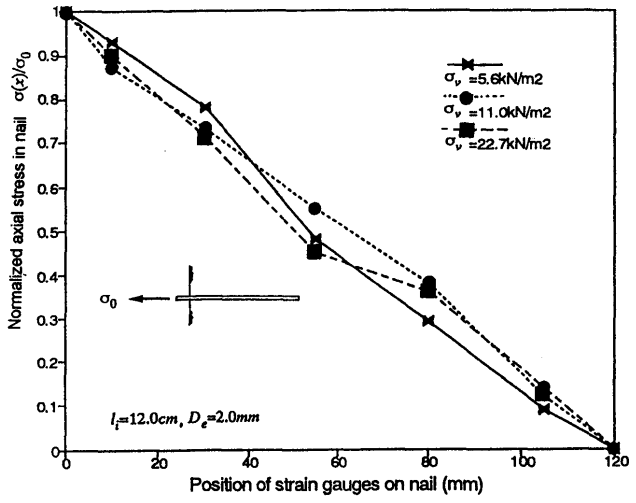

Fig. 6. **variation of axial stress along stiff rough nails in pull-out tests**

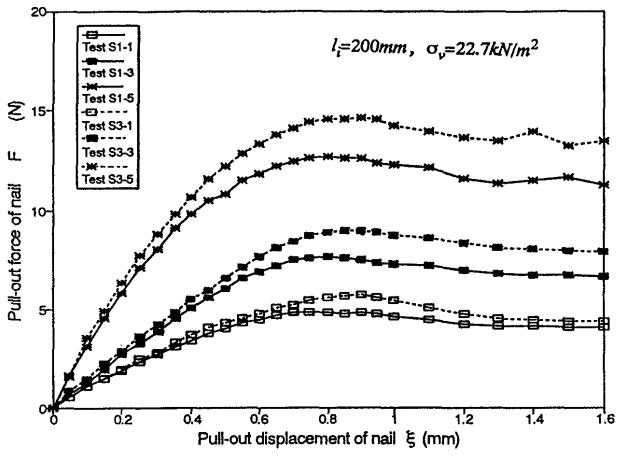

Fig. 8. **Force/displacement curves for pull-out tests with stiff smooth nails**

and the applied vertical surcharge stress was about 23 kPa. Compared with the data from the stiff-rough nails, much smaller peak pull-out forces were observed and the displacements required to mobilize F_p were $\xi_p=0.8\sim0.9$ mm irrespective of the type of sand, which is less than half of those for the rough nails. After reaching its peak value, the pull-out force first gradually reduced and then became nearly constant at a nail displacement of about $\xi=1.4$ mm for 14/25 dense sand and $\xi=1.2$ mm for 50/100 dense sand. The apparent friction coefficients and corresponding angles of interface (bond) friction δ_b ($=\tan^{-1}f^*$) were $f^*=0.26$ ($\delta_b=14.5°$) for 50/100 dense sand and $f^*=0.32$ ($\delta_b=17.7°$) for 14/25 dense sand. These observed values of δ_b are considerably smaller than the critical state friction angle of quartz sand $\phi_{cv}=33°\sim35°$ (Bolton, 1986), and further, even smaller than the angle of mineral-to-mineral friction angle ϕ_u estimated by Chen and Liu (1990) assuming $\phi_{cv}=34°$, as

$$\phi_u=\frac{(\phi_{cv}-22.5°)}{0.9}+15.0°=26.7° \qquad (6)$$

In the design of reinforced soil walls using steel or concrete strips with smooth surfaces, Schlosser and Guilloux (1979) suggested that the apparent friction coefficient of the reinforcement is approximately equal to $f^*=0.40$ ($\delta_b=22°$). As the surface of the smooth nails used in the current pull-out tests were very smooth, their suggestion for f^* is considered reasonable. During pull-out of smooth reinforcement, a discontinuity can be formed at the interface by the soil particles sliding on the reinforcement surface (Gourc and Beech, 1989); whereas with rough surfaces a dilating shear zone some 20 particles thick forms in the sand around the nail.

It was also observed that, unlike with the rough nails which are discusssed later, the apparent friction coefficients f^* of smooth nails were nearly constant irrespective of the diameter D of the nail, as shown in Fig. 9.

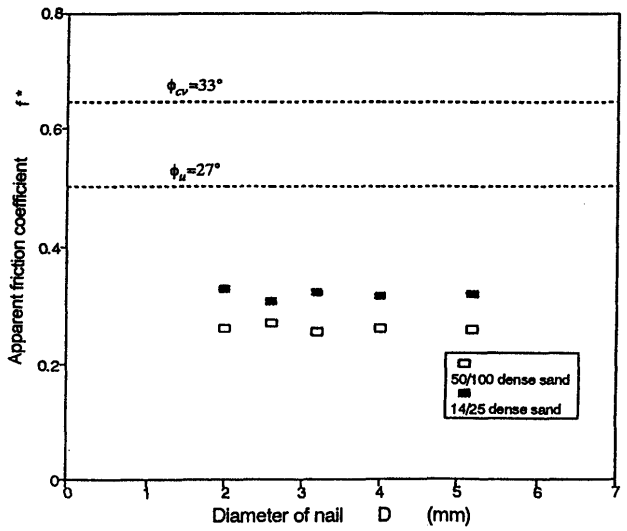

Fig. 9. Pull-out tests of stiff smooth nails: influence of nail diameter

Pull-out Tests of Extensible-Rough nails

Figure 10 shows the load-displacement results for extensible-rough nails, which were made of a small rubber tube; test details are given in Table 4. The initial length of a nail was always 200 mm while the surcharge stress was about 23 kPa. Tests were performed using 50/100 dense (Test F1-1), 50/100 medium dense (Test F2-1) and 14/25 dense (Test F3-1) Leighton Buzzard Sands. The results for the extensible nail are significantly different from those for the stiff nails; the peak pull-out forces F_p are smaller, and the pull-out displacements ξ_p required to mobilize F_p two or three times larger. The apparent friction coefficients are $f^*=1.88$ and 2.10 for 50/100 dense and medium dense sands respectively, and 2.47 for the 14/25 sand. The reduction in pull-out force after reaching peak was much greater than with the stiff-rough nails. It should be noted that the Poisson's ratio effect in the extensible nail would tend to cause a reduction in contact stress between nail and sand.

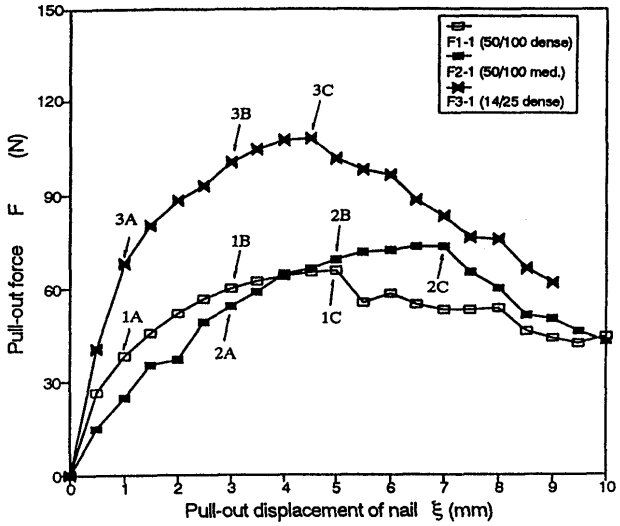

Fig. 10. Force/displacement curves for pull-out tests with extensible rough nails

Table 4. Details of pull-out tests with extensible rough nails

Test	Nail length l (mm)	Diameter D (mm)	Surcharge σ_v (kPa)	Peak force F_p (N)	f^*	μ^*
Test with dense 50/100 L.B. sand						
F1-1	200	3.7	22.7	65.4	1.88	2.32
Test with medium dense 50/100 L.B. sand						
F2-1	200	3.7	22.7	73.1	2.10	2.89
Test with dense 14/25 L.B. sand						
F3-1	200	5.0	23.2	107.9	2.47	2.22

ANALYSIS

Soil-nail Interface Stiffness and Axial Stresses in Nails

Theoretical considerations

Adib (1988), Jaber (1989) and Farmer (1975), from model tests and finite element analyses, have shown that in a pull-out test of a nail the maximum pull-out force and the shear stress distribution along the nail are greatly influenced by the interface stiffness k_i, where

$$\tau = k_i \xi \tag{7}$$

defines the relationship between the shear stress τ on a nail and the pull-out displacement ξ.

In order to investigate the influence of the interface stiffness k_i in a pull-out test, consider a simple circular nail/soil model, as shown in Fig. 11. It is assumed that both the nail and soil are elastic and the surrounding soil is subjected only to shearing in the x-direction, (Farmer, 1975). Longitudinal equilibrium of the element of the nail gives

$$\frac{d\sigma(x)}{dx} = -\frac{2}{R_a}\tau(x) \tag{8}$$

$$\sigma(x) = -E_a \frac{d\xi(x)}{dx} \tag{9}$$

in which R_a is the radius of the nail, $\tau(x)$ and $\sigma(x)$ are the shear and axial stresses, E_a is the elastic modulus of the nail, and $\xi(x)$ is its pull-out displacement. When the displacement $\xi(x)$ of the nail is small and the surface of the nail is assumed to be rough, then the displacement $\eta(x)$ of the soil in contact with the nail surface may be regarded as equal to that of the nail (Jewell, 1980). Then

$$\xi(x) = \eta(x) = \int_{R_a}^{R^{a+h}} \gamma(y)dy = \int_{R_a}^{R^{a+h}} \frac{\tau(x,y)}{G(\gamma)}dy \tag{10}$$

where h is the current thickness of the deforming (or rupture) zone and G and γ are the shear modulus and shear strain of the sand, respectively. Assuming that the shear stress $\tau(x, y)$ varies with $1/y$ in the cylindrical zone of displacements within the sand,

$$\tau(x,y) = \{\tau(x)\}_{y=R_a}\frac{R_a}{y}, \quad R_a \le y \le R_a + h \tag{11}$$

The interface stiffness k_i is derived by combining Eqs. (7), (10) and (11)

$$k_i = \frac{1}{R_a}\frac{1}{\int_{R_a}^{R_a+h}\frac{dy}{G(\gamma)y}} \tag{12}$$

If it is assumed that the shear modulus G of the soil is constant irrespective of the shear strain γ, then Eq. (12) is simplified as

$$k_i = \frac{1}{R_a}\frac{G}{\ln\left(1+\frac{h}{R_a}\right)} \tag{13}$$

Figure 12 shows the relationship between (k_i/G) and the radius R_a of a nail estimated from Eq. (13) for various thicknesses of the deforming zone h. The thickness of this deforming zone is likely to be in the range of 10–20 times the mean particle diameter of the soil. As the radius R_a and the thickness h increase, the magnitude of (k_i/G) becomes smaller. While large changes of (k_i/G) are observed for smaller values of R_a, (k_i/G) is nearly constant for $R_a \ge 3$ cm. In the design of pipe lines, for which the radius is usually larger than that of a nail, a range of $(k_i/G) = 1 \sim 3$ has been proposed by several researchers (e.g. Hmadi et al., 1988), and this range of (k_i/G) is consistent with the results shown in Fig. 12.

Stiff nails

Although the interface stiffness k_i is simply modelled by Eq. (13) in idealized conditions, the difficulty of obtaining the thickness h of the deforming zone and the shear modulus G of the soil still remains. Therefore, the interface stiffness k_i may be determined more reliably by experiment. In a pull-out test of a stiff nail, the interface stiffness k_i can simply be calculated using Eq. (7) since the shear stress τ and the pull-out displacement ξ are

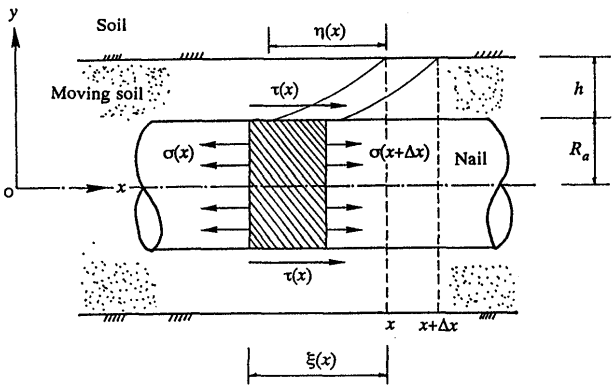

Fig. 11. Nail-soil interaction model

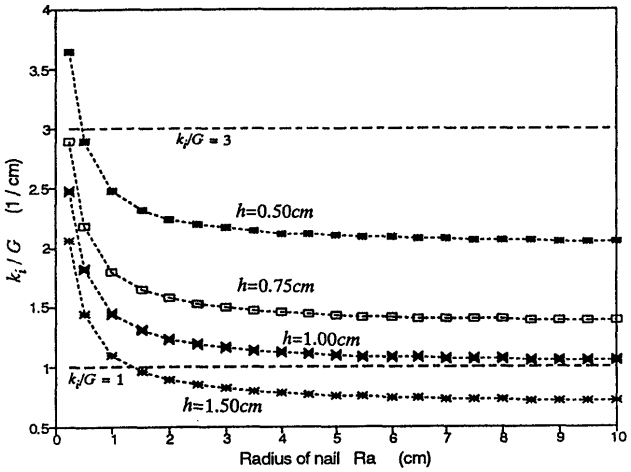

Fig. 12. Relations between interaction parameter and nail radius

almost constant along the nail. In this case the axial stress in the nail will simply vary linearly along its length, as found experimentally.

As noted above, the load-displacement curve for pull-out tests with stiff rough nails may be approximately modelled by a hyperbola up to the peak pull-out force F_p. The interaction parameter k_i for a range of pull-out displacements $0 \leq \xi \leq \xi_p$ is then given as

$$k_i(\xi) = \frac{1}{a + b\xi} \tag{14}$$

Parameters a and b are obtained from the load-displacement curves by plotting the pull-out data as ξ/τ versus ξ.

Extensible nails

For extensible nails, Eqs. (7), (8) and (9) may be combined to give (Farmer, 1975):-

$$\frac{d^2\xi(x)}{dx^2} = \frac{2k_i}{R_a E_a}\xi(x) = \alpha^2 \xi(x) \tag{15}$$

where α is defined by:

$$\alpha = \sqrt{\frac{2k_i}{R_a E_a}} \tag{16}$$

The boundary conditions for Eq. (15) with regard to the axial stress in a nail are given at the head ($\sigma_x = \sigma_0$) and at the end ($\sigma_x = 0$). By using Eq. (9) and these boundary conditions, the general solutions for Eq. (15) are:

$$\frac{\sigma(x)}{\sigma_0} = \frac{\sinh\{\alpha(l-x)\}}{\sinh(\alpha l)}, \tag{17}$$

$$\frac{\xi(x)}{\xi_0} = \frac{\cosh\{\alpha(l-x)\}}{\cosh(\alpha l)} \tag{18}$$

where ξ_0 is the displacement at the head of the nail ($x = 0$). Figure 13 shows the solutions of Eq. (17) for different values of the relative stiffness α. As α decreases, or as the relative stiffness between the nail and soil increases for nails of the same diameter D, the axial stress distribution $\sigma(x)/\sigma_0$ becomes more linear and the shear stress distribution becomes more constant along the nail.

If the assumption is made that the value of k_i locally for an extensible-rough nail is the same as for a stiff-rough nail in the same sand, the values of k_i obtained from the latter may be used to predict the behaviour during pull-out of the former.

Thus from Eqs. (14), (15) and (16),

$$\frac{d^2\xi(x)}{dx^2} = \alpha^2\xi(x) = \frac{4D_e\xi(x)}{E_a(D_e^2 - D_i^2)\{\alpha + b\xi(x)\}} \tag{19}$$

where $D_e = 0.3$ cm and $D_i = 0.2$ cm are the external and internal diameters, and $E_a = 0.02$ kN/m^2 is the elastic modulus of the rubber nail. Parameters a and b for the hyperbolae from the tests with the stiff-rough nails of almost the same diameter, at the same surcharge stress σ_v and in the same sand, were obtained as follows:-

$a = 0.022$ cm^3/N and $b = 0.120$ cm^2/N for 50/100 dense sand,

$a = 0.030$ cm^3/N and $b = 0.145$ cm^2/N for 50/100 medium dense sand, and

$a = 0.009$ cm^3/N and $b = 0.102$ cm^2/N for 14/25 dense sand.

Equation (19) may be solved numerically, with appropriate boundary conditions. Typical calculated values of the normalised displacements along the nail, for three different stages of the test with the extensible nail in 50/100 dense sand, are shown in Fig. 14.

It is clear that much of the pull-out displacement $\xi(x)$ and shear stress $\tau(x)$ is generated near the head of the nail ($x = 0$), while at small pull-out forces, such as at stage A (*see* Fig. 10), there are negligible displacements of the nail deeper into the soil. As the pull-out displacement ξ_0 or pull-out force F increases, the displacement distributions $\xi(x)$ are gradually transmitted to the nail deeper in the soil, as pointed out by Gourc and Beech (1989) for the case of pull-out of a geotextile in sand. It is also apparent that a considerable pull-out displacement at the head of the nail will be needed to mobilize the friction along the full length of the extensible nail. The results imply that for a pull-out test of an extensible nail,

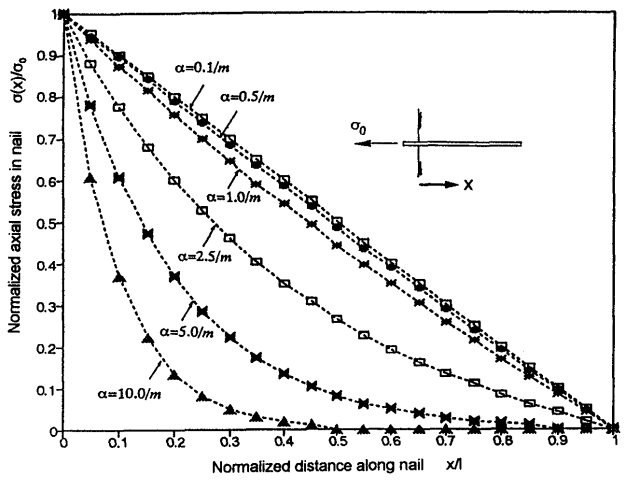

Fig. 13. Axial stress distributions in a nail as a function of the parameter α.

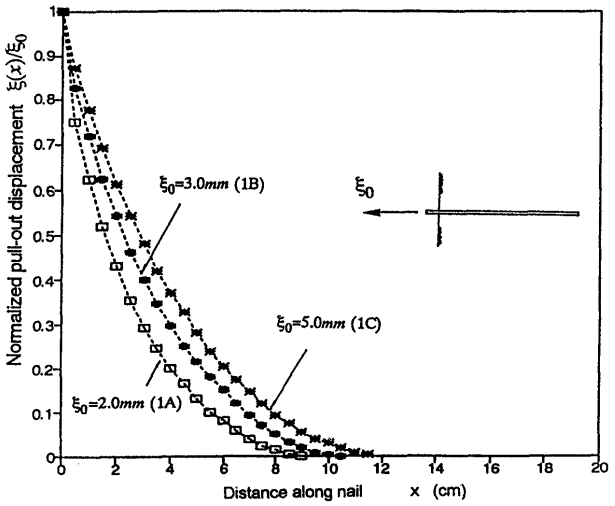

Fig. 14. Normalised pull-out displacements of extensible nails

the peak pull-out force F_p is not directly proportional to the length of the nail, in contrast to a stiff nail.

However, since the hyperbolae with parameters a and b cannot exactly model the post peak pull-out curves, (e.g. reduction of the pull-out force F after the peak), the analysis based on Eq. (19) tends to overestimate the shear stress τ on the extensible nail, particularly near its head ($x=0$). For example, when peak pull-out forces F_p are observed in the tests, the analysis suggests that friction is only mobilised along half the length of the nail. From this point of view, it is important for the analysis of friction of an extensible nail to formulate correctly the pull-out curve of the stiff nail to include the post peak behaviour, so as to model correctly the progressive failure of the nail.

There must also be some doubt concerning the assumption that k_i is the same locally for stiff and extensible nails under the same conditions. For the former, the axial strain in the soil adjacent to the nail must be zero, and the mobilized friction angle is that in direct shear, while for an extensible nail this condition no longer holds. However the analysis above is sufficient to emphasise the difficulty of calculating pull-out resistance, and of analysing pull-out tests, for nails with significant axial extensibility.

Peak Pull-out Force for Stiff Rough Nails

Experimental results

The values of f^* are clearly likely to be different for soils with different friction angles. When comparing pull-out test results in different soils, a more appropriate parameter for describing the friction of a nail may be the friction coefficient μ^*, defined above as

$$\mu^* = \frac{f^*}{\tan \phi_{ds}} = \frac{F_p}{\pi D l \sigma_m \tan \phi_{ds}} \tag{20}$$

where ϕ_{ds} is the direct shear friction angle.

Figures 15(a) and (b) show the relationships between the friction coefficient μ^* and the diameter D and normalized diameter D/D_{50} from the pull-out tests of stiff-rough nails. D_{50} is the mean particle size of the sand. The figures also include a data point for stiff-rough nails in dense 14/25 Leighton Buzzard sand conducted by Jewell (1980), showing good agreement with the other results. The friction coefficient μ^* gradually decreases as the diameter D increases, although μ^* was shown above to be almost constant irrespective of the diameter for smooth nails (Fig. 9). The effect of D/D_{50} on the friction coefficient μ^* is significant for D/D_{50} in the range $1 \sim 35$, but the effect appears to diminish for higher values, which are more normal in the field.

It is easy to imagine that the pull-out of a nail, especially of a rough nail, causes stress changes in dense sand due to dilatancy of the soil, and hence increases the peak pull-out force F_p as reported by Johnston and Romstad (1989) from large scale pull-out tests of reinforcement. Similarly, Yazici and Kaiser (1992) reported that a larger bore hole diameter leads to a reduced normal stress σ_m and bond strength τ for cable bolts embedded in rock, because the dilatancy effect is decreased as the diameter of the borehole becomes larger. Houlsby (1991), using cavity expansion theory, clearly showed that a pile of larger diameter exhibits less friction resistance than a smaller pile due to soil dilatancy. Significant increases of normal stresses on steel piles were reported by Hettler (1992) and Lehane et al. (1993) for model tests and in-situ pile loading tests, respectively. Schlosser and Elias (1978) also demonstrated that the effect of the restricted dilatancy of the soil on the peak pull-out force F_p of a nail is significant, and values of apparent friction coefficient F^* of up to 7.0 or friction coefficient μ^* up to 6.3 were reported from their pull-out tests of ribbed strips. Heymann et al. (1992) performed a number of in-situ pull-out tests of nails of diameters from $D=20$ mm to 30 mm in various ground conditions. They showed that the majority of the values of friction coefficient lay within a range of $\mu^*=2 \sim 4$, which bounds quite well the test data in Fig. 15. They emphasized the importance of soil dilatancy in predicting the maximum pull-out force of a nail.

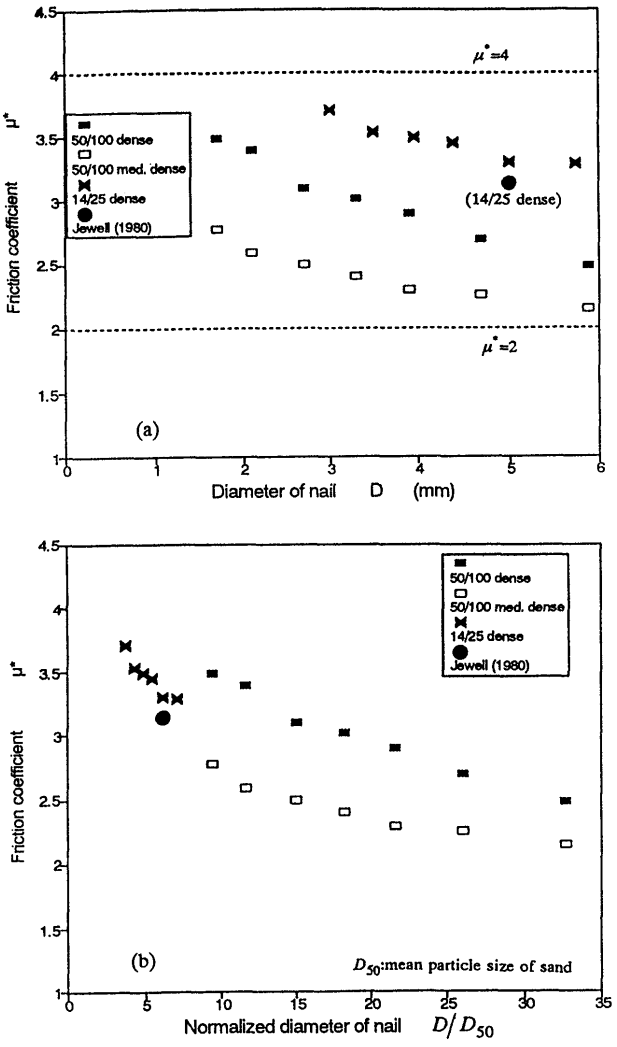

Fig. 15. Pull-out tests of stiff rough nails; influence of nail diameter: (a) friction coefficient plotted against nail diameter, (b) friction coefficient plotted against normalised nail diameter

Figures 16(a), (b) and (c) show the relationships between the mobilized friction coefficient μ^*_{mob} and the pull-out displacement ξ of the stiff-rough nails, where

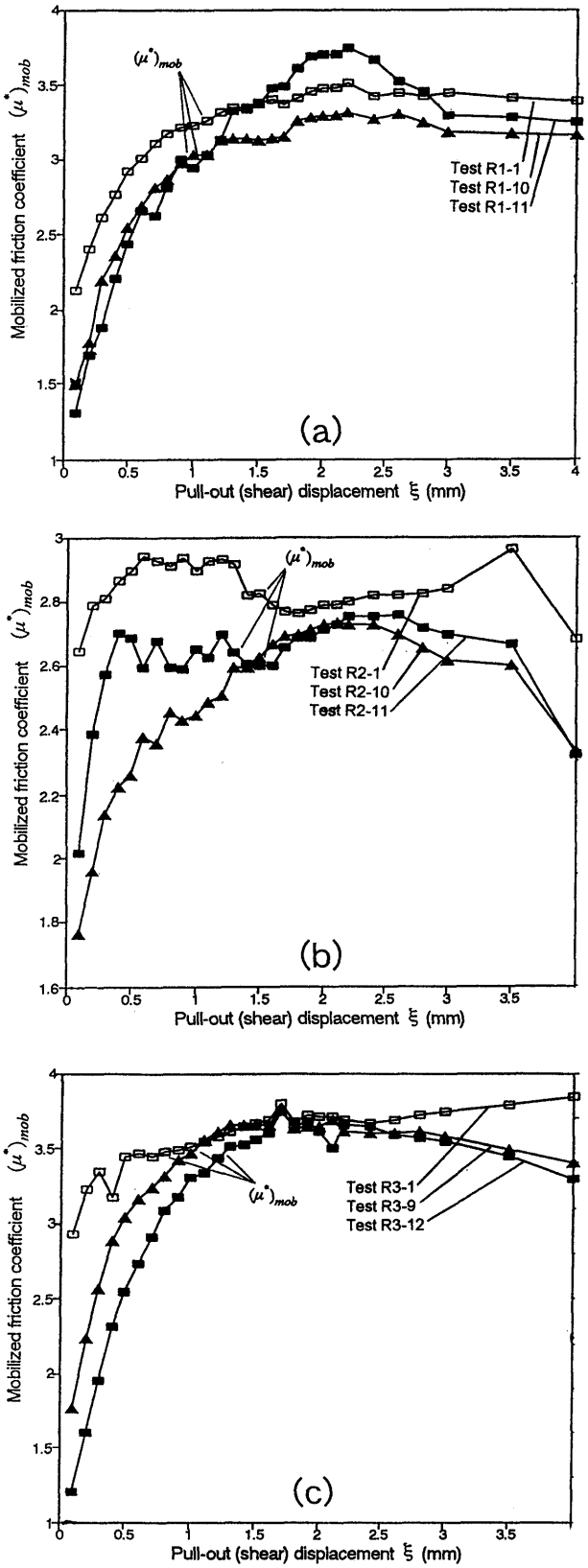

Fig. 16. Mobilised friction coefficients and pull-out displacements: (a) in 50/100 dense sand, (b) in 50/100 medium dense sand, (c) in 14/25 dense sand

$$\mu^*_{mob}=\frac{f^*_{mob}}{\tan(\phi_{ds})_{mob}} \tag{21}$$

Even from the early stages of pull-out displacement, the mobilized friction coefficient μ^*_{mob} is observed to be always greater than 1.0. This suggests that even for small shear strains of the soil, the soil dilates and the normal stress σ_m on the nail increases, in contrast to boundary measurements in direct shear tests which often exhibit a contraction in the early stages of the test. However, Palmeira (1987) measured the shear strain and volumetric strain at the central plane in direct shear tests, and reported that dense 14/25 Leighton Buzzard sand dilates from shear strains of 1 to 2%, as shown in Fig. 17. In the pull-out tests, assuming that the shear zone around the nails is some 15–20 particles thick, a displacement of 0.1 mm represents a shear strain in the sand of about 3% for 50/100 sand and 0.8% for 14/25 sand.

Theoretical effects of dilation

If the mean normal stress on a nail is increased from σ_m to $(\sigma_m+\Delta\sigma_m)$ due to soil dilatancy during pull out, then

$$\mu^*=1+\frac{\Delta\sigma_m}{\sigma_m} \tag{22}$$

From elastic cavity expansion theory (Boulton et al., 1986; McGown et al., 1989), the radial stress change results in a displacement of the soil mass Δh and

$$\Delta\sigma_m=2G\Delta\varepsilon=\frac{2G\Delta h}{D+h} \tag{23}$$

in which $\Delta\varepsilon$ is the increment of the circumferential strain of the soil, h is the thickness of the shear zone, Δh is the increment of shear zone thickness due to the dilatancy of soil, and G is the shear modulus of the soil. Combining

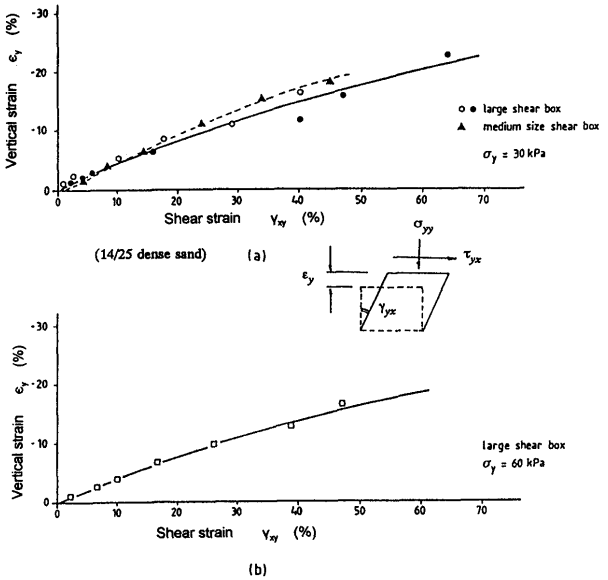

Fig. 17. Mean vertical strain (dilation) against shear strain in direct shear tests (after Palmeira, 1987)

Eqs. (22) and (23) gives:

$$\mu^* = 1 + \frac{2G}{\sigma_m}\frac{\Delta h}{(D+h)} = 1 + \frac{2G}{\sigma_m}\frac{\Delta h/D_{50}}{(D/D_{50}+h/D_{50})} \quad (24)$$

Equation 24 conceptually shows the increase of the friction coefficient μ^* from the direct shear friction angle ϕ_{ds} due to the increased normal stress $\Delta\sigma_m$ in the pull-out tests. While rotation of the principal stress in the soil is not considered in Eq. (24), Symes (1983) pointed out that for dense sand the effect of rotation of the principal stress on the friction on a pile is not significant. The important features of Eq. (24) are:-

(1) as observed in the pull-out tests, the friction coefficient μ^* decreases as the diameter D of the nail increases; the additional normal stress $\Delta\sigma_m$ on a nail due to the dilatancy sharply decreases as D increases, particular for smaller values of D.
(2) for diameters $D \geq 20$ mm, the friction coefficient μ^* can be assumed nearly constant; for nail diameters generally used in practice, μ^* may extrapolate to about 2.
(3) the friction coefficient μ^* is closely related to the dilation of the soil; when there is no dilation in the sand, so that $\psi = \Delta h = 0$, then this leads to $\mu^* = 1$ and $f^* = \tan\phi_{ds}$.
(4) the friction coefficient μ^* increases as the normalized shear modulus G/σ_m increases; thus μ^* is influenced by both the strength and stiffness of the soil.

From Eq. (24), it is hypothesized that

$$\mu^* = fn\left(\frac{G}{\sigma_m}, \frac{h}{D}, \frac{\Delta h}{D}\right) = fn\left(\frac{G}{\sigma_m}, \frac{D_{50}}{D}, \psi\right) \quad (25)$$

where it is also assumed in Eq. (25) that the thickness h of the shear zone and the increase in radius Δh of the shear zone are a function of the mean particle size D_{50} and angle of dilation ψ of the soil, respectively.

APPLICATION IN PRACTICE

The primary aim of the small-scale tests reported in this paper was to obtain pull-out data for the model nails for use in the analysis of centrifuge tests of model nailed slopes (Tei et al., 1997). While the theoretical background and general trends presented here should be relevant to full scale nails, direct extrapolation of experimental results to the field situation should be treated with caution. Significant differences between model tests and full-scale nails are:-

(a) the installation procedures for the nails are quite different, and will result in different initial stresses at the nail-soil interface and in the soil close to the nail.
(b) relative size effects between the nail diameter and soil mean particle diameter may be significant in the model tests, tending to increase the apparent stiffness and strength of the soil.
(c) stress levels in the model nail tests were quite low; soil friction angles and the effects of dilation are likely to be greater in the model tests than in typical field situations.

Points (b) and (c) in particular are likely to lead to lower apparent friction coefficients between nail and soil in the field than in the model tests; however, pressure grouting of full scale nails may compensate by inducing higher initial contact stresses between nail and soil.

CONCLUSIONS

A comprehensive series of pull-out tests of model soil nails in dry sand has been performed. The apparent friction coefficients (bond) between stiff 'rough' nails and soil were shown to be dependent on the strength (friction angle) of the soil, but also on the rate of dilation during shear, the stiffness of the soil, and the diameter of the nail in relation to the particle size of the soil. For grouted nails of common diameters in dilatant fine-grained soils, the value of μ^* may be over 2.0, while in non-dilatant soils the pull-out resistance must be based on the measured nail-soil interface friction angle without any increase in normal stress.

Typical displacements to mobilise peak pull-out resistance in dense and medium dense sand were about 2 mm. This is probably related to the surface roughness, and values of about half this were obtained for the smooth nails. The curves of pull-out resistance against displacement were approximately hyperbolic in shape up to peak, and such curves were used to predict deflections of nailed walls in centrifuge tests (Tei et al., 1997).

For smooth nails the interface friction angle is much smaller and there is negligible increase in normal stress on the nail due to dilation of the soil. It is clear that smooth nails (where the soil/nail interface is significantly less rough than a soil/soil interface) should be avoided in practice.

For relatively extensible nails the situation is complicated by the possibility of progressive failure, field tests will be difficult to back-analyse, and design should be based on large-displacement or critical state values of interface friction between nail and soil.

ACKNOWLEDGEMENT

The authors are grateful to the Tokyu Construction C. Ltd of Japan for the leave of absence and financial support for Kouji Tei to pursue research at Oxford University.

REFERENCES

1) Adib, M. E. (1988): "Internal lateral earth pressure in earth walls," Ph. D. Thesis, Univ. of California at Berkeley.
2) Airey, D. W. (1987): "Some observations on the interpretation of shear box test results," Internal Report CUED/D-SOILS/TR 196, Univ. of Cambridge.

3) Bergado, D. T., Chai, J. C. and Balasubramanan, A. S. (1992): "Interaction between grid reinforcement and cohesive-frictional soil," Proc. of Int. Symp. on Earth Reinforcement Practice, Fukuoka, Vol. 1, pp. 29–34.
4) Bolton, M. D. (1986): "The strength and dilatancy of sands," Géotechnique, Vol. 36, No. 1, pp. 219–226.
5) Bolton, M. D. (1990): "Reinforced soil: Laboratory testing and modelling," Proc. of the Int. Reinforced Soil Conf., Glasgow, pp. 287–298.
6) Boulton, M., Plytas, C. and Foray, P. (1986): "Comportement de interface et prevision du frottement lateral le long des pieux, et tirants de ancrage," Revue Francaise de Geotechnics, Vol. 2, pp. 31–48.
7) Chang, J. C., Hannon, J. B. and Forsyth, R. A. (1977): "Pull resistance and interaction of earth work reinforcement and soil," Transport Research Record No. 640, Washington, USA.
8) Chen, W. F. and Liu, X. L. (1990): "Limit analysis in soil mechanics," Developments in Geotech. Engrg., Elsevier, 52.
9) Dunham, R. K. (1976): "Anchorage tests on strain gauged resin bounded bolts," Tunnels and Tunnelling, Vol. 8, No. 6, pp. 73–76.
10) Farmer, I. W. (1975): "Stress distribution along a resin-grouted rock anchor," J. of Int. Rock Mech. Min. Sci. and Geomech., Vol. 12, pp. 347–351.
11) Gourc, J. P. and Beech, J. F. (1989): "Soil-reinforcement interaction. Contribution to discussion," Proc. of Int. Conf. on SMFE, Rio de Janeiro, Vol. 4, pp. 3007–3008.
12) Hettler, A. (1992): "Approximation formula for piles under tension," Proc. of IUTAM Conf. on Deformation and Failure of Granular Material, Delft, pp. 603–608.
13) Heymann, G., Rohde, A. Schwarz, K. and Friedlaender, E. (1992): "Soil nail pull out resistance in residual soils," Proc. of the Int. Symp. on Earth Reinforcement Practice, Fukuoka, Vol. 1, pp. 487–496.
14) Hmadi, E. K. and O'Rourke, M. J. (1988): "Soil Springs for Buried Pipeline Axial Motion," Proc. ASCE, J. of Geotech. Engrg., Vol. 114, No. 11, p. 1335.
15) Houlsby, G. T. (1991): "How the dilatancy of soils affects their behaviour," Invited Lecture, 10th Eur. Conf. on SMFE, Florence.
16) Ingold, T. S. and Templeman, J. E. (1979): "The comparative performance of polymer net reinforcement," Proc. of Int. Conf. on the Reinforcement of Soils, Paris, Vol. 1, pp. 65–70.
17) Jaber, M. B. (1989): "Behaviour of reinforced soil walls in centrifuge model tests," Ph. D. Thesis, Univ. of California at Berkeley.
18) Lehane, B. M., Jardine, R. J., Bond, A. J. and Frank, R. (1993): Mechanics of shaft friction in sand from instrumented pile tests," Proc. ASCE, J. of Geotech. Engrg., Vol. 119, No. 1, pp. 19–34.
19) Jewell, R. A. (1980): "Some effects of reinforcement on the mechanical behaivur of soils," Ph. D. Thesis, Univ. of Cambridge.
20) Jewell, R. A. (1989): "Direct shear tests in sand," Géotechnique, Vol. 39, No. 2, pp. 309–322.
21) Jewell, R. A. and Wroth, C. P. (1987): "Direct shear tests on reinforced sands," Géotechnique, Vol. 37, No. 1, pp. 53–68.
22) Johnston, R. S. and Romstad, K. M. (1989): "Dilatation and boundary effects in large scale pull-out tests," Proc. of 12th Int. Conf. on SMFE, Rio de Janeiro, Vol. 2, pp. 1263–1266.
23) McGown, A., Murray, R. T. and Jewell, R. A. (1989): "State-of-the-Art Report on reinforced soil," Proc. 12th Int. Conf. on SMFE, Rio de Janeiro, Vol. 4, pp. 2637–2648.
24) Murray, R. T., Carder, D. R. and Krawczyk, J. V. (1979): "Pull-out tests on reinforcements embedded in uniformly graded sand subjected to vibration," Proc. 7th Eur. Conf. on SMFE, Brighton, Vol. 3, pp. 115–120.
25) Palmeira, E. M. (1987): "The study of soil-reinforcement interaction by means of large scale laboratory tests," D. Phil. Thesis, Univ. of Oxford.
26) Palmeira, E. M. and Milligan, G. W. E. (1989): "Scale and other factors influencing the results of grids buried in sand," Géotechnique, Vol. 39, No. 3, pp. 511–524.
27) Pedley, M. J. (1991): "The performance of soil reinforcement in bending and shear," D. Phil. Thesis, Univ. of Oxford.
28) Schlosser, F. (1990): "Mechanically stabilized earth retaining structures in Europe. Design and performance of earth retaining structures," ASCE Geotechnical Special Publication, p. 347–377.
29) Schlosser, F. and Elias, V. (1978): "Friction in reinforced earth," ASCE, Convention, Pittsburgh, USA.
30) Schlosser, F. and Guilloux, A. (1979): "Le frottement sol-armature dans les ouvrages en Terre Armee," Proc. Int. Conf. on Soil Reinforcement, Paris, Vol. 1.
31) Symes, M. J. (1983): "Rotation of principal stresses in sand," Ph. D. Thesis, Imperial College, Univ. of London.
32) Tei, K. (1993): "A study of soil nailing in sand," D. Phil. Thesis, Univ. of Oxford.
33) Tei, K., Taylor, R. N. and Milligan, G. W. E. (1997): "Centrifuge model tests of nailed soil slopes," (Accepted for publication by Soils and Foundations.)
34) Yazici, S. and Kaiser, P. K. (1992): "Bond strength of grouted cable bolts," Int. J. of Rock Mech. Min. Sci. and Geomech., Vol. 29, No. 3, pp. 27–29.